Low-Field Optically Detected EPR Spectroscopy of Transient Photoinduced Radical Pairs

Christopher T. Rodgers, Kevin B. Henbest, Philipp Kukura,† Christiane R. Timmel,* and P. J. Hore*

Department of Chemistry, University of Oxford, Physical and Theoretical Chemistry Laboratory, Oxford OX1 3QZ, U.K.

Received: February 13, 2005; In Final Form: April 26, 2005

The effects of simultaneously applied weak static and weak radio frequency magnetic fields on the recombination of transient (<100 ns) radical pairs have been investigated using a low-field optically detected electron paramagnetic resonance technique. Measurements on the photoinduced electron-transfer reaction of perdeuterated pyrene with 1,3-dicyanobenzene using a ∼0.3 mT radio frequency field at three separate frequencies (5, 20, and 65 MHz) in the presence of 0−4 mT static fields yield spectra that are strikingly sensitive to the frequency of the time-dependent field, to the strength of the static field, and to the relative orientation of the two fields. The spectra are simulated using a modified form of the γ-COMPUTE algorithm originally devised for calculating magic angle spinning NMR spectra of polycrystalline samples. The essential features of the spectra are consistent with the radical pair mechanism and were satisfactorily simulated using parameters whose values are either known independently or for which estimates are readily available. The calculations included hyperfine couplings to four deuterons in the pyrene cation radical and three protons in the 1,3-dicyanobenzene anion radical. Spin-selective recombination was modeled using an exponential distribution of radical encounter times. The results are discussed in the context of the proposal that radical pair chemistry forms the basis of the magnetoreceptor that allows birds to sense the Earth's magnetic field as a source of compass information during migration.

Introduction

Radical pairs are important reaction intermediates in a wide range of photolytic, thermal and radiolytic processes.[1,2] Their electron spin-dependent reactivity and magnetic interactions give rise to magnetic polarization phenomena observable by nuclear magnetic resonance (NMR) and electron paramagnetic resonance (EPR) spectroscopies.[3−5] Radical pairs also form the basis of the only well-established mechanism—the radical pair mechanism—by which magnetic fields are known to influence the rates and yields of chemical reactions.[6,7] These phenomena have been widely exploited to provide detailed insight into free radical chemistry and physics,[8,9] photosynthetic energy conversion,[10] the structure and folding of proteins,[11] and enzyme kinetics.[6,12,13]

Chemical reactions such as bond homolysis, electron transfer, or hydrogen abstraction usually create radicals in pairs, with correlated electron spins. The two unpaired electron spins, one on each radical, are initially either parallel (a triplet state) or antiparallel (a singlet state), according to the spin multiplicity of the precursor(s). The chemistry of radical pairs is controlled not only by their diffusive motions in solution and their inherent reactivity but also, crucially, by the spin-correlation via the requirement to conserve spin angular momentum. For example, a triplet pair would be unable to recombine to give a diamagnetic product, unless it could first transform into a singlet state. Coherent oscillatory interconversion of singlet and triplet states is driven by intramolecular electron−nuclear hyperfine interactions, a process that is sensitive to the presence of applied magnetic fields, offering a tool to influence and probe the yields and kinetics of radical reactions. A weak ($\lesssim$1 mT) magnetic field typically enhances the efficiency of singlet ↔ triplet interconversion (the so-called low field effect[14,15]). For a singlet-born radical pair, therefore, a weak field reduces the probability of recombination from the singlet state, and consequently boosts the number of free radicals that escape from the solvent cage into the bulk solution.[14−16]

Although modern time-resolved EPR techniques are versatile and powerful,[5] it is often less than straightforward to study radical pairs directly, principally because of their transient nature (typical lifetimes are 10−100 ns). Furthermore, despite the enormous nonequilibrium electron spin polarization with which the radical pairs are created, such experiments suffer from the limited sensitivity associated with detecting low energy microwave photons. These considerations, together with the need to understand more fully the details of radical−radical interactions and dynamics in solution, led us to devise a new technique for the direct observation of short-lived radical pairs, a form of optically detected zero-field EPR.[17−22] It differs from more conventional EPR techniques in two important respects: the strong static magnetic field, normally required to polarize the electron spins, is dispensed with and magnetic resonance is detected optically via the reaction yield. This experiment thus entails radio frequency (RF) excitation of transitions in the radical pair between energy levels split only by hyperfine interactions in order to perturb the singlet ↔ triplet interconversion and so to modify the yield of the reaction product(s)

* To whom correspondence should be addressed at the Department of Chemistry, University of Oxford, Physical and Theoretical Chemistry Laboratory, South Parks Road, Oxford OX1 3QZ, U.K. E-mail: (P.J.H.) peter.hore@chem.ox.ac.uk; (C.R.T.) christiane.timmel@chem.ox.ac.uk. Telephone: (P.J.H.) +44 1865 275415; (C.R.T.) +44 1865 275156. Fax: +44 1865 275410.

† Present address: Department of Chemistry, University of California, Berkeley, CA 94720.

10.1021/jp050765z CCC: $30.25
Published on Web 05/25/2005

SCHEME 1: Simplified Photochemical Reaction Scheme for Pyrene and 1,3-Dicyanobenzene[a]

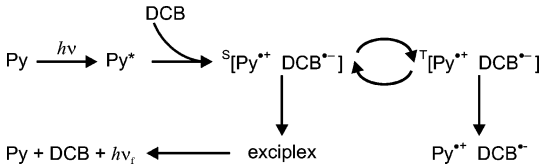

[a] S and T indicate singlet and triplet states of the radical pair; Py* is the excited singlet state of pyrene. The curved arrows represent the coherent interconversion of singlet and triplet radical pairs by hyperfine and electron Zeeman interactions. Magnetic field effects on radical recombination were detected via the exciplex fluorescence ($h\nu_F$). The free radicals that escape from the geminate radical pair eventually undergo back electron transfer to regenerate Py and DCB.

formed from the singlet state. The technique is closely related to RYDMR (reaction yield detected magnetic resonance) in which (usually microwave) EPR transitions are excited between states split by the Zeeman interaction with a strong static magnetic field.[23−25]

These studies are extended here to investigate the combined effects of weak static and weak RF fields on radical pair electron-transfer reactions. We describe the results of experiments on the photoinduced electron-transfer reaction between perdeuterated pyrene (Py-d_{10}) and 1,3-dicyanobenzene (DCB) in solution using a ∼0.3 mT RF field at three frequencies (5, 20, and 65 MHz) in the presence of 0−4 mT static fields, varying the relative orientations of the two fields. The spectra are simulated using a modified form of the γ-COMPUTE algorithm devised for the calculation of magic angle spinning NMR spectra of polycrystalline samples.[26−28] Some preliminary low-field optically detected EPR spectra of radical pairs have been presented in ref 29.

Experimental Methods

Magnetic field effects on the recombination of photoinduced radical ion pairs were detected as described previously[18−21] via exciplex fluorescence, as summarized in Scheme 1 for the reaction of pyrene with 1,3-DCB. Radical pairs were produced by continuous UV illumination. Singlet pairs can recombine to produce the fluorescent exciplex state while triplet pairs diffuse apart to form free radicals. Applied static and oscillating magnetic fields affect the extent and frequency of singlet−triplet interconversion and so alter the fraction of radical pairs that form exciplexes, which in turn results in a change in the fluorescence intensity. The continuous RF field was 100% amplitude-modulated (at 381 Hz) and the exciplex fluorescence was demodulated and recorded using phase-sensitive detection. The static magnetic field was supplied by water-cooled Helmholtz coils placed around both the sample cell and the RF coils which could, together, be rotated with respect to the static field to allow the orientation dependence of the EPR spectrum to be measured. A flow system was used to avoid sample photodegradation. The strength of the RF field was estimated to be ∼0.3 mT.[29] Samples were not shielded from the geomagnetic field because this additional, very small (∼50 μT), static field is expected to have a negligible effect on the radical pair recombination, a conclusion that is supported by the insensitivity of the observed fluorescence intensity to small (∼100 μT) changes in the applied static field (see below).

Experiments were performed on a solution of 5×10^{-4} M Py-d_{10} and 10^{-2} M 1,3-DCB in 9:1 cyclohexanol:acetonitrile at room temperature.

Theoretical Methods

We consider a spin-correlated radical pair evolving under the influence of (1) isotropic electron−nuclear hyperfine interactions and (2) the isotropic Zeeman interactions of the electron spins with (a) a static magnetic field of strength $B_0 = \omega_0/\gamma_e$ and (b) a linearly polarized radio frequency field of peak strength $B_1 = \omega_1/\gamma_e$ and frequency $\omega_{RF}/2\pi$ (γ_e is the magnetogyric ratio of the electron). The coherent evolution of the radical pair, described by a spin density operator $\hat{\rho}(t)$, is governed by the spin Hamiltonian (in angular frequency units)

$$\hat{H}(t;\gamma) = \sum_{j=1}^{2}\{\sum_{k=1}^{N} a_{jk}\hat{\mathbf{S}}_j\cdot\hat{\mathbf{I}}_k + \omega_1\hat{S}_{jx}\sin(\omega_{RF}t + \gamma) + \omega_0[\hat{S}_{jz}\sin\theta + \hat{S}_{jx}\cos\theta]\} \quad (1)$$

in which j and k label the electron and nuclear spins respectively, $\hat{\mathbf{S}}_j$ and $\hat{\mathbf{I}}_k$ are electron and nuclear spin angular momentum operators, a_{jk} are the hyperfine coupling constants, t is the time after the formation of the radical pair, θ is the angle between the two magnetic fields, and γ is the phase of the RF field at $t = 0$. If the nuclear spin space is of dimension M ($= 2^N$ for N spin-$^1/_2$ nuclei), $\hat{H}(t;\gamma)$ is represented by a $4M \times 4M$ Hermitian matrix. Anisotropic magnetic interactions are assumed to be averaged by molecular motion. Spin evolution arising from the difference in the two electronic g-values and from the nuclear Zeeman interactions is negligible at the magnetic field strengths considered (≤4 mT). We assume that the exchange and dipolar interactions between the radicals and all spin relaxation processes may be neglected.

Concurrent with their spin evolution, the two radicals undergo rapid translational motions and are assumed to recombine in a diffusion-controlled manner whenever they encounter in a singlet state but to be mutually unreactive in the triplet state. We treat this reaction−diffusion process using the "exponential model"[15,30] in which the two radicals of a spin-correlated pair undergo a single encounter, with a distribution of encounter times given by $f(t) = ke^{-kt}$ where k is a first-order rate constant. The total probability that the radical pair recombines (the "singlet yield") is the integral over t of the probability that the encounter occurs at time t multiplied by the probability $\langle\hat{P}^S\rangle(t)$ that the radical pair is in a singlet state at the moment of encounter:[15]

$$\Phi_S = \int_0^\infty \langle\hat{P}^S\rangle(t) f(t) dt \quad (2)$$

The expectation value of the singlet projection operator $\hat{P}^S$ is given by

$$\langle\hat{P}^S\rangle(t) = \mathrm{Tr}[\hat{\rho}(t)\hat{P}^S] = \frac{1}{M}\mathrm{Tr}[U^\dagger(t,0;\gamma)\hat{P}^S U(t,0;\gamma)\hat{P}^S] \quad (3)$$

in which the radical pair is assumed to be formed in a singlet state ($\hat{\rho}(0) = \hat{P}^S/M$) and $U(t,0;\gamma)$ is the spin evolution propagator for the interval $0 \rightarrow t$ and initial phase γ.

In the experiments described here, radical pairs are formed by continuous illumination in the presence of a continuous RF field. A given pair may therefore be created, with equal likelihood, at any point during a cycle of the RF field. In other words, Φ_S must be averaged over a uniform distribution of γ in the interval $0 \rightarrow 2\pi$. Approaches to this calculation are complicated by the time dependence of the spin Hamiltonian: as the RF field is linearly polarized, comparable in strength to both the static field and the hyperfine couplings, and not necessarily perpendicular to the static field, the familiar rotating frame transformation[31] is not applicable. Instead, we exploit the

properties of $\hat{H}(t;\gamma)$ to perform a time-dependent calculation over a single cycle of the RF field.

The important symmetries here are the periodicity of the RF field and the fact that the initial phase can be treated as a time-shift (m is an integer):

$$\hat{H}(t;\gamma) = \hat{H}(t + 2m\pi/\omega_{RF};\gamma)$$
$$\hat{H}(t;\gamma) = \hat{H}(t + \gamma/\omega_{RF};0) \quad (4)$$

Mathematically similar properties are encountered in magic angle spinning (MAS) NMR, in which a rapidly rotating polycrystalline sample with anisotropic magnetic interactions is subject to a sequence of RF pulses such that the spin system evolves under a time-dependent Hamiltonian.[28,32−36] Furthermore, the random orientation of the crystallites means that the calculated response must be averaged over an ensemble of orientations ("carousel averaging"[37]). Unless done carefully, this averaging may seriously diminish the performance and hence the feasibility of the calculations. The magnetic resonance literature contains several articles devoted to efficient methods for carrying out such calculations.[26,27,38,39] Here we adapt the γ-COMPUTE (calculation over one modulation period using time evolution with γ-averaging) algorithm as formulated by Hohwy et al.,[27] where γ is one of the three Euler angles that relate the crystallite orientation to the MAS rotor axis system.

As described above, to simulate magnetic field effects, we must first calculate the time-dependent singlet probability using eq 3. The propagator $U(T,0;\gamma)$ acting over one period T of the RF field is of central importance; it is related to the average Hamiltonian $\bar{H}$, by

$$U(T,0;\gamma) = \exp[-i\int_0^T \hat{H}(t;\gamma)\mathrm{d}t] = \exp(-i\bar{H}T) \quad (5)$$

It is easily shown that $\bar{\omega}_r$, the eigenvalues of $\bar{H}$, are independent of the initial phase γ.

We evaluate the integral in eq 5 by approximation using an n-strip trapezium rule, equivalent to assuming that $\hat{H}$ is piecewise constant in each interval T/n.[27] Following Hohwy et al.,[27] after some manipulations we arrive at the following expression for the Fourier transform of $\langle\hat{P}^S\rangle(t)$

$$\langle\hat{P}^S\rangle(\omega) = \sum_{r,s}^{4M}\sum_{k=-n/2}^{n/2-1} \bar{a}_{rs}^{(k)}\delta(\omega - \bar{\omega}_{rs} - k\omega_{RF}) \quad (6)$$

In other words, for each pair of eigenstates r,s of $\bar{H}$, there is a group of n contributions to the singlet probability with frequencies centered around the difference in energy between the states, $\bar{\omega}_{rs} = \bar{\omega}_r - \bar{\omega}_s$, and spaced by the radio frequency ω_{RF}. The amplitudes of the peaks are given by $\bar{a}_{rs}^{(k)} = |q_{rs}^{(k)}|^2$ where $q_{rs}^{(k)}$ is defined by eq 27 of ref 27.[40]

Finally, combining eqs 2 and 6, we obtain

$$\Phi_S = \sum_{r,s}^{4M}\sum_{k=-n/2}^{n/2-1} \bar{a}_{rs}^{(k)}F(\bar{\omega}_{rs} + k\omega_{RF}) \quad (7)$$

where $F(\omega)$, the Fourier transform of $f(t)$, is given by

$$F(\omega) = \frac{k^2}{k^2 + \omega^2} \quad (8)$$

for the exponential model.

Calculations were performed in Matlab. Although converged values of Φ_S were obtained for $n = 16$, all simulations presented below were done with $n = 64$. The following hyperfine couplings were included in the simulations (Scheme 2): in 1,3-DCB$^{\bullet-}$, a group of 2 protons ($a = 0.829$ mT) and a single proton ($a = 0.144$ mT)[41] and in Py-$d_{10}^{\bullet+}$, a group of 4 deuterons (spin quantum number $I = 1$, $a = 0.083$ mT).[42] Smaller couplings in both radicals were neglected (Scheme 2). The symmetries associated with equivalence among the nuclear spins were exploited where appropriate. With these values, the average hyperfine interactions, defined as[21,43]

SCHEME 2: ^{1}H, ^{2}H, and ^{14}N Hyperfine Coupling Constants (mT) in the Py-$d_{10}^{\bullet+}$ and 1,3-DCB$^{\bullet-}$ Radicals

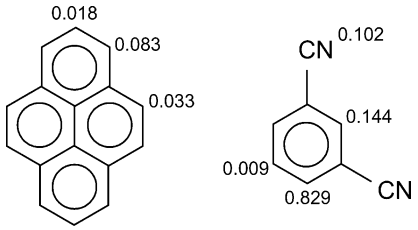

$$\langle a\rangle = \sqrt{\sum_k a_k^2 I_k(I_k + 1)} \quad (9)$$

are 0.235 mT for Py-$d_{10}^{\bullet+}$, 1.02 mT for 1,3-DCB$^{\bullet-}$, and 1.05 mT for the radical pair as a whole. The corresponding EPR frequencies are 6.6, 28.6, and 29.4 MHz, respectively.

In summary, the following modifications to the γ-COMPUTE algorithm[27] were made: (a) the calculation is set up in the laboratory frame of reference rather than in an axis system rotating in step with the RF field; (b) the periodicity of the spin Hamiltonian arises from the interaction of the electron spins with the RF field rather than the modulation of anisotropic NMR interactions by sample spinning; (c) the integral over the powder angle γ becomes an average over the phase of the RF field at the moment of creation of the radical pair; (d) instead of the NMR spectrum, we compute the singlet product yield using the exponential model. We believe this type of approach, which seems not to have been used before in the context of spin chemistry, is an attractive alternative to "brute force" methods in situations where the rotating frame transformation is invalid. Some preliminary results of the approach have recently been published.[29]

Results

A. Preliminary Simulations. Some aspects of the effect of a RF field on the yield of a radical pair reaction can be seen from the calculations in Figure 1A, which model a radical pair comprising Py-$d_{10}^{\bullet+}$ and 1,3-DCB$^{\bullet-}$. Performed with $k = 4.0 \times 10^7$ s^{-1}, $\omega_{RF}/2\pi = 5$ MHz and $\theta = 0$ (parallel static and RF fields), these simulations show the dependence of the singlet yield Φ_S on B_0 for values of B_1 between 0 and 1 mT.

Several features are apparent. The low field effect, visible as a minimum in Φ_S at $B_0 \approx 0.25$ mT, is abolished by the RF field when B_1 is stronger than ~0.3 mT. The magnitudes of the changes in Φ_S produced by the two fields acting alone are roughly similar; for example, relative to $B_0 = B_1 = 0$, the reduction in Φ_S caused by $B_0 = 0.2$ mT (with $B_1 = 0$) is very similar to that arising from $B_1 = 0.2$ mT (with $B_0 = 0$). There is no obvious resonance at or near the field where the RF would be in resonance with the electron Zeeman splitting ($B_0 = 0.18$ mT). A strong resonance is expected[23−25] when the radio frequency is much larger than the hyperfine couplings, as discussed later.

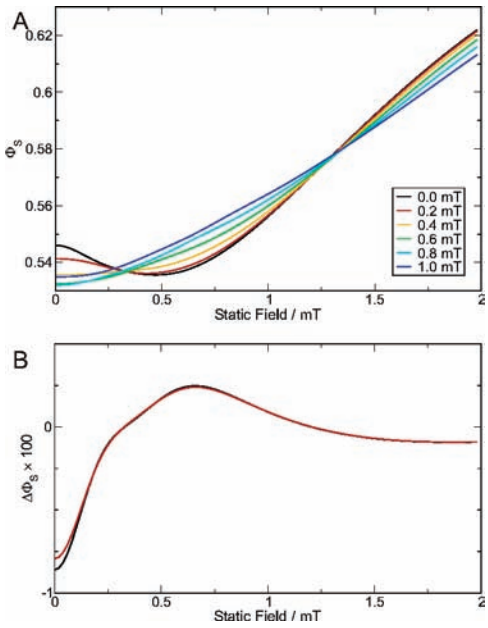

Figure 1. (A) Simulated effects of simultaneously applied parallel static and RF magnetic fields on the Py-d_{10}•+/1,3-DCB•− radical pair, $k = 4.0 \times 10^7$ s^{-1}, $\omega_{RF}/2\pi = 5$ MHz and $\theta = 0$. The singlet yield is plotted as a function of B_0 for values of B_1 between 0.0 and 1.0 mT. (B) Change in the singlet yield produced by a 0.3 mT RF field calculated under the same conditions as in part A. The result of exact numerical integration over one cycle of the RF field (black) is compared with simple subtraction, $\Phi_S(B_1) - \Phi_S(0)$ (red).

Each of the curves in Figure 1A was calculated using a single value of B_1, in contrast to the experimental data which were recorded with 100% amplitude modulation of the RF field (at 381 Hz). With typical lifetimes of 10−100 ns, each radical pair experiences an almost constant peak RF field; if the fluorescence intensity is linear in B_1, one could therefore account for the modulation simply by subtracting the singlet yield calculated for $B_1 = 0$ from that calculated using the peak RF field strength. One such curve is shown in Figure 1B (for $B_1 = 0.3$ mT and all other parameters as in Figure 1A) together with the response generated by numerically integrating Φ_S over one cycle of the sinusoidal audio frequency modulation. Despite the nonlinear dependence of Φ_S on B_1 evident in Figure 1A, the differences between the two curves are slight; henceforth we use exclusively the much faster subtraction method.

B. Experimental Measurements. Figure 2 shows experimental (left-hand side) and calculated (right-hand side) spectra for the Py-d_{10}/1,3-DCB reaction at three radiofrequencies: 5 MHz (top), 20 MHz (middle) and 65 MHz (bottom), chosen to be respectively smaller than, comparable to, and larger than the average hyperfine interaction in the radical pair. The principal features of the experimental data are discussed in the following paragraphs.

The effect of the RF field depends strongly on its frequency. At 65 MHz, a dominant peak appears close to the usual high-field EPR resonance condition arising from the electron Zeeman interaction (∼0.036 mT MHz^{-1}, i.e., ∼2.3 mT). The shoulders and satellite peaks, approximately 0.8 mT either side of the central resonance, arise from the largest hyperfine coupling in the radical pair (two equivalent protons with $a = 0.829$ mT in 1,3-DCB•−). Essentially similar spectra can be expected for radiofrequencies higher than 65 MHz, with correspondingly stronger static fields, except that the signal strength will depend more strongly on the relative orientation of the two magnetic fields and the asymmetry in the hyperfine structure should disappear. In the high field limit, where the static field B_0 is much stronger than all hyperfine interactions, no signal is expected for parallel B_0 and B_1 fields.[44−48] For the weaker B_0 fields used here, the selection rules for allowed RF transitions are less restrictive with the result that parallel and perpendicular transitions have comparable intensity.[27,44−48]

The responses for parallel and perpendicular fields also have comparable amplitudes at the two lower radiofrequencies. The shape of the signal as a function of B_0 is most sensitive to the relative orientation of the two fields at 20 MHz, reflecting the comparable size of the hyperfine interactions (∼1.0 mT), the B_0 field required for the Zeeman resonance (0.71 mT), and the B_1 field strength (∼0.3 mT). The θ dependence is less complex at 5 MHz, at which frequency the Zeeman resonance ($B_0 = 0.18$ mT) is obscured by resonances with hyperfine splittings. In the absence of a dominant Zeeman interaction, there is no clear spin quantization axis in the laboratory frame leading to a less pronounced orientation dependence of the spectra. At all three frequencies the signals are weak for $B_0 > 4$ mT, when the RF is off-resonance with respect to both Zeeman and hyperfine interactions.

With the exception of the 65 MHz data, it is difficult to rationalize the form of the observed spectra using physical arguments familiar from conventional EPR and RYDMR spectroscopies. Outside of the high-field limit, the distribution of spin energy levels and the probabilities of RF-induced transitions between them become highly complex. Numerical simulations are therefore indispensable in this low-field regime if sense is to be made of the observed spectra.

The simulations shown on the right-hand side of Figure 2 were performed using the adapted γ-COMPUTE algorithm with the literature values of hyperfine coupling constants quoted above, a recombination rate constant $k = 4 \times 10^7$ s^{-1} and a RF field strength $B_1 = 0.3$ mT. Beyond choosing physically plausible values of the last two parameters, no attempt has been made to optimize the resemblance to the experimental data. The agreement at each of the three frequencies, while clearly not perfect, is nonetheless striking. All the major features of the experimental spectra are reproduced in the simulations at approximately correct B_0 field positions. This correspondence is particularly satisfying given the complexity of the spin systems, the approximate treatment of the radical diffusion and the very limited number of variable parameters. Perhaps the most dramatic discrepancy between theory and experiment is seen at 5 MHz for $B_0 < 0.5$ mT where the simulated signals are quite strongly negative in contrast to the experimental intensities which are close to zero. This difference probably stems from excluding the smaller hyperfine interactions in the two radicals. In our earlier study of chrysene with isomers of DCB, in which only the four nuclei with the largest couplings were included, the simulated intensities for $B_0 < 0.5$ mT were much more eccentric than they are here.[29]

Finally, it is apparent that at certain B_0 fields (∼0.9 mT at 5 MHz and ∼1.5 mT at 20 MHz), the exciplex fluorescence is independent of θ. Although the origin of this effect is unclear, it is reassuring to see similar features in the simulations.

C. Further Simulations. Although the values of k and B_1 used for the simulations presented in Figure 2 are physically plausible, their values are not known precisely. The value of the rate constant k, in particular, is to some extent ill-defined because it parameterizes an approximate model of the radical encounters (viz. the exponential model). It is therefore important to investigate the sensitivity of the simulated spectra to the values of these two quantities.

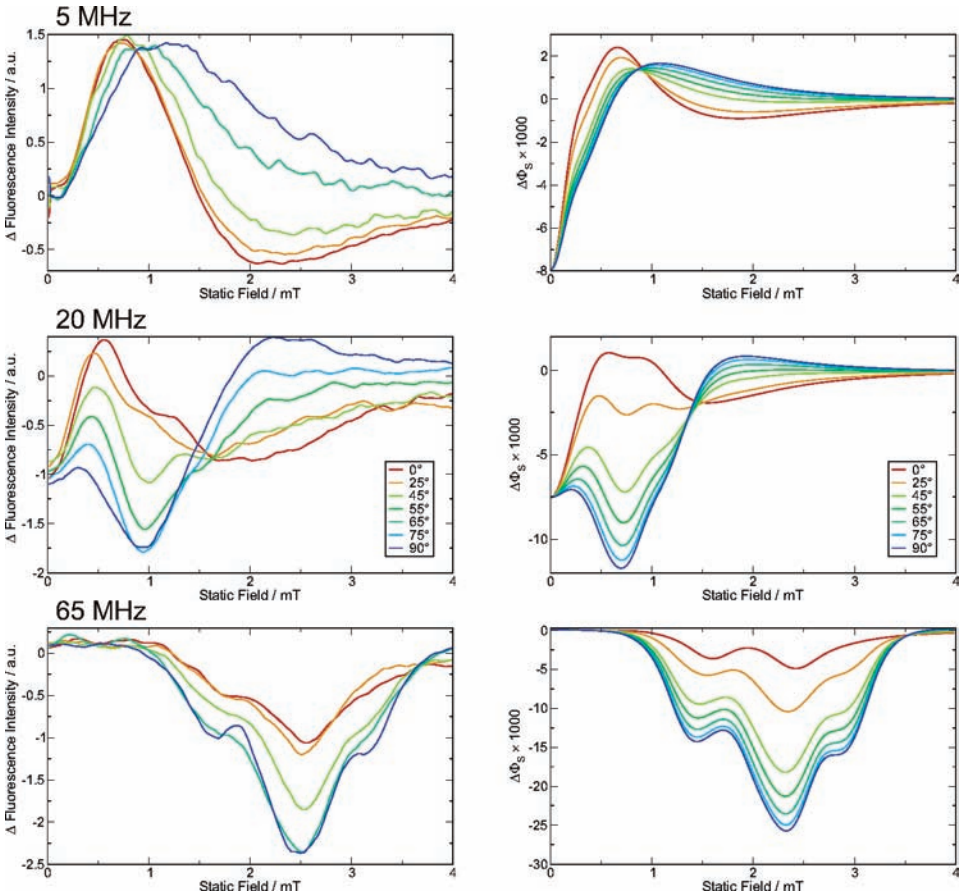

Figure 2. Experimental (left) and simulated (right) low-field optically detected EPR spectra of Py-$d_{10}^{\bullet+}$/1,3-DCB$^{\bullet-}$ at radiofrequencies 5 MHz (top), 20 MHz (middle) and 65 MHz (bottom). Values of θ are as indicated. The simulations were performed using $B_1 = 0.3$ mT and $k = 4 \times 10^7$ s^{-1}. The experimental spectra represent the changes in the exciplex fluorescence produced by the radio frequency field.

Figure 3 shows calculations for $k = 2 \times 10^7$ s^{-1}, 4×10^7 s^{-1}, and 6×10^7 s^{-1} and $B_1 = 0.3$ and 0.5 mT for $\omega_{RF}/2\pi = 20$ MHz, the frequency for which the spectra are expected to be most sensitive to k and B_1. Overall, comparison of Figure 3 with the experimental spectra in Figure 2 suggests that the values of k and B_1 used for the simulations in Figure 2 are probably close to optimum. Similar calculations for $\omega_{RF}/2\pi = 5$ and 65 MHz (not shown) bear substantially less resemblance to the experimental data when $k = 2 \times 10^7$ s^{-1} and are not much different from Figure 2 for $k = 6 \times 10^7$ s^{-1} or for $B_1 = 0.5$ mT.

It appears to be impossible to rationalize in any simple way the shapes of the simulated signals in Figure 3. They reflect, in a highly complex manner, the resonances between the RF field and the energy levels arising from the hyperfine and electron Zeeman interactions. They are further complicated by the fact that the B_1 field is not weak enough to be considered as merely probing without perturbing the energy level splittings produced by the intrinsic magnetic interactions.

A little more light can be shed on the form of the spectra at the lowest radio frequency (5 MHz). With typical radical pair lifetimes in the range 10−100 ns, there will come a point, as ω_{RF} is progressively decreased, where the strength of the RF field does not alter perceptibly on the time scale of radical pair recombination. In this low-frequency limit, we may approximate the spectra by treating the RF field as an additional contribution to the *static* field, and averaging over a suitable ensemble of radical pairs to account for the random phase γ. Thus, the effective static field varies between the extreme values of $|B_0 - B_1|$ and $B_0 + B_1$ when $\theta = 0$ and between B_0 and $\sqrt{B_0^2+B_1^2}$ when $\theta = 90°$. Figure 4 shows that this approach provides a reasonable approximation to the exact calculations shown in the top right-hand panel in Figure 2. Differences between the two sets of simulations are noticeable, but not pronounced. Further calculations (not shown) suggest that the low-frequency limit is essentially exact for this particular choice of k, B_1 and hyperfine couplings, provided the radio frequency is less than about 1 MHz; i.e., the radical pair lifetime is less than ∼3% of the period of the RF irradiation.

Discussion

It is clear from the above that the low-field optically detected EPR spectra of transient ($\lesssim$100 ns) radical pairs can be strikingly sensitive to the weak applied magnetic fields needed to record them. The response of the reaction product yield to the linearly polarized RF field depends in a complex manner not only on its frequency and on the strength of the applied static magnetic field, but also on the relative orientation of the two fields. One can anticipate that the polarization of the RF field (i.e., linear or circular) will also influence the observed spectra. The spectra are thus a rich source of information on the kinetics, motions and relaxation of the radicals, reflecting the comparable magnitude of the relevant magnetic fields—applied static, applied RF, and intrinsic hyperfine. Simpler, less potentially informative spectra would no doubt be observed in various limiting cases, none of which is generally applicable here: the static field is not strong enough for the high field approximation to be valid; neither field is weak enough to be treated or thought of as a perturbation; and the radio frequency is for the most part too

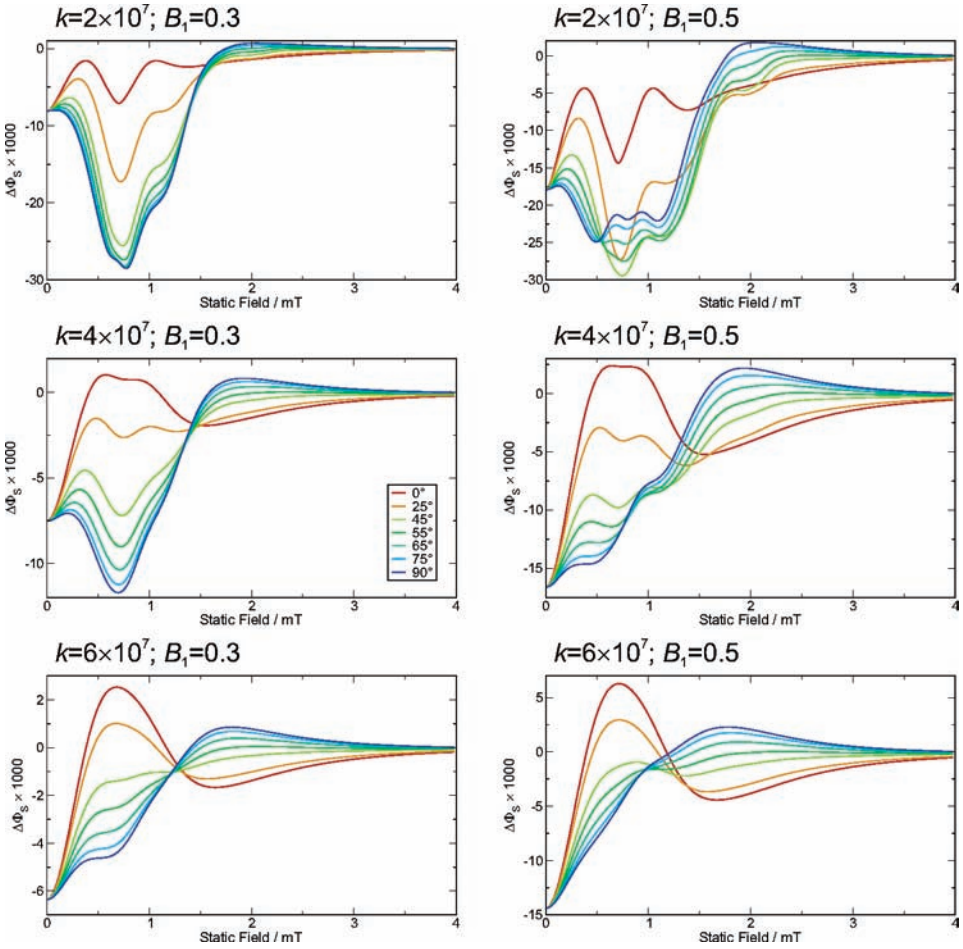

Figure 3. Simulated low-field optically detected EPR spectra of Py-$d_{10}^{\bullet+}$/1,3-DCB$^{\bullet-}$ at a radio frequency of 20 MHz. $B_1 = 0.3$ mT (left) and 0.5 mT (right). $k = 2 \times 10^7$ s^{-1} (top), 4×10^7 s^{-1} (middle), and 6×10^7 s^{-1} (bottom). Values of θ are as indicated.

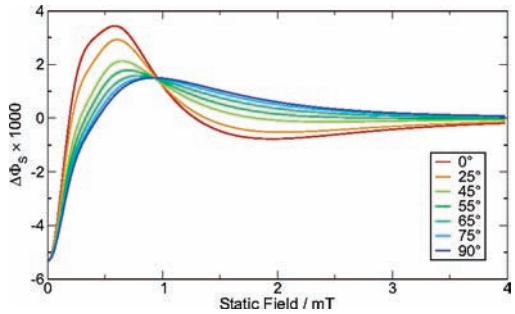

Figure 4. Approximate, simulated low-field optically detected EPR spectra of Py-$d_{10}^{\bullet+}$/1,3-DCB$^{\bullet-}$ at a radio frequency of 5 MHz. The simulations were performed by treating the RF field as invariant during a radical pair lifetime. Values of θ are as indicated. $B_1 = 0.3$ mT and $k = 4 \times 10^7$ s^{-1}.

high for the RF field to be effectively static on the time scale of radical recombination.

The customary approaches to simulating such spectra, based on the rotating frame transformation, are not applicable. Instead, we have adapted from solid-state NMR a numerical approach (γ-COMPUTE) valid for a periodic but otherwise arbitrary spin Hamiltonian. In this way, we have shown that the essential features of the spectra are consistent with the radical pair mechanism (RPM) and can be satisfactorily simulated using parameters whose values are either known independently or for which reasonable estimates are readily available. The calculations are efficient enough that it should be possible to extract quantitative information from the spectra by fitting suitable models of the radical motion, or even to invert the data to obtain the reencounter probability distribution $f(t)$ directly. Unlike the approach of Canfield et al.,[49,50] in which the interaction with the oscillating magnetic field is treated as a perturbation on the hyperfine and Zeeman interactions (B_0), γ-COMPUTE is exact whatever the magnitude of B_1. It is therefore to be preferred in the present case where B_0, B_1, and the hyperfine couplings are of comparable size.

The agreement between the simulated and experimental spectra although clearly not perfect is most encouraging. Despite its simplicity, the exponential model—combined with the assumptions of diffusion control, singlet-only reactivity and a single encounter for all radical pairs—appears to be an excellent basis for understanding the complex field and orientation dependence of the spectra. As noted above, the correspondence between theory and experiment could be improved by the inclusion in the calculations of a few more of the smaller hyperfine couplings, perhaps by treating them semiclassically.[43,51]

The absence of obvious resonances at or near the B_0 field at which the radio frequency matches the electron Zeeman splitting in the spectra with $\omega_{RF}/2\pi = 5$ MHz in Figure 2 is seemingly at variance with Canfield et al.[49] who predicted a sharp "Zeeman resonance" for a one-proton radical pair with a long lifetime subject to a very weak radio frequency field (see ref 49, Figure 5). The origin of this discrepancy has been clarified by further calculations (not shown). When the frequency of the RF field is comparable to the hyperfine couplings, a Zeeman resonance only occurs when one of the two radicals has no hyperfine couplings, such that its energy levels are split *only* by the

interaction with the applied static field. Even in this special case, such a resonance is only observable if the recombination rate constant k and the radio frequency field strength B_1 are sufficiently small that it is not obscured by other (hyperfine) resonances and/or by line broadening. Canfield's result is thus for a rather special case which does not apply here.

As discussed elsewhere,[29] the sensitivity of the chemical response to simultaneously applied static and oscillatory magnetic fields could form the basis of a diagnostic test for the operation of the RPM. This might be valuable in the context of magnetic field effects in complex (e.g., biological) systems in which the identities and properties of any radicals involved might be completely unknown. The unique features of radical pair reactions are that, as well as responding to an applied static field, they should (a) also be sensitive to the frequency and direction of an additional RF field of comparable intensity and (b) exhibit a Zeeman resonance at a frequency that is not strongly dependent on the hyperfine interactions provided they are weaker than the static field required for resonance ($\sim$0.036 mT MHz^{-1}).

Finally, radical pair chemistry has been proposed as the basis of the magnetoreceptor that allows birds to sense the Earth's magnetic field as a source of compass information during migration.[52−55] This interesting suggestion has very recently received strong support from the observation that European robins become disoriented when a radio frequency field (0.1−10 MHz) as weak as 85 nT is superimposed on the Earth's field (46 μT).[56] The disorienting effect of the RF field was found to depend on the relative orientation of the two fields. It is not yet clear exactly how our experiments on radicals free to undergo rapid rotational tumbling relate to the situation required for an avian magnetoreceptor where the radical pairs would need to be immobile with definite orientation with respect to the animal's head. Nevertheless, it would appear from the complexity of the responses observed here, that radical pair chemistry offers considerable scope for evolutionary optimization of a sensitive magnetoreceptor. The extreme sensitivity of the robins' response to a RF field two orders of magnitude weaker than the Earth's field, suggests a resonant interaction, perhaps with specific hyperfine splittings in one of the radicals. Such effects have not been observed in our experiments which, in general, show similar sensitivity to static and RF fields.

Acknowledgment. We are grateful to the EMF Biological Research Trust, the Royal Society, the Human Frontier Science Program and the EPSRC for support.

References and Notes

(1) Steiner, U. E.; Ulrich, T. *Chem. Rev.* **1989**, *89*, 51−147.
(2) Hayashi, H. *Introduction to Dynamic Spin Chemistry*; World Scientific Publisher: Singapore, 2004.
(3) Goez, M. *Concepts Magn. Reson.* **1995**, *7*, 69−86.
(4) Goez, M. *Adv. Photochem.* **1997**, *23*, 63−163.
(5) Murai, H.; Tero-Kubota, S.; Yamauchi, S. *Electron Paramagn. Reson.* **2000**, *17*, 130−163.
(6) Grissom, C. B. *Chem. Rev.* **1995**, *95*, 3−24.
(7) Brocklehurst, B. *Chem. Soc. Rev.* **2002**, *31*, 301−311.
(8) Woodward, J. R. *Prog. React. Kinet. Mech.* **2002**, *27*, 165−207.
(9) Tanimoto, Y.; Fujiwara, Y. In *Handbook of Photochem. Photobiol.*, Vol. 1, *Inorganic Photochemistry*; Nalwa, H. S., Ed.; American Scientific Publishers: Stevenson Ranch, CA, 2003; pp 413−446.
(10) Volk, M.; Ogrodnik, A.; Michel-Beyerle, M. E. In *Anoxygenic Photosynthetic Bacteria*; Blankenship, R. E., Madigan, M. T., Bauer, C. E., Eds.; Kluwer; Dordrecht, The Netherlands, 1995; p 595.
(11) Mok, K. H.; Hore, P. J. *Methods* **2004**, *34*, 75−87.
(12) Harkins, T. T.; Grissom, C. B. *Science* **1994**, *263*, 958−960.
(13) Taraban, M. B.; Leshina, T. V.; Anderson, M. A.; Grissom, C. B. *J. Am. Chem. Soc.* **1997**, *119*, 5768−5769.
(14) Brocklehurst, B.; McLauchlan, K. A. *Int. J. Radiat. Biol.* **1996**, *69*, 3−24.
(15) Timmel, C. R.; Till, U.; Brocklehurst, B.; McLauchlan, K. A.; Hore, P. J. *Mol. Phys.* **1998**, *95*, 71−89.
(16) Eveson, R. W.; Timmel, C. R.; Brocklehurst, B.; Hore, P. J.; McLauchlan, K. A. *Int. J. Radiat. Biol.* **2000**, *76*, 1509−1522.
(17) Timmel, C. R.; Hore, P. J. *Chem. Phys. Lett.* **1996**, *257*, 401−408.
(18) Woodward, J. R.; Jackson, R. J.; Timmel, C. R.; Hore, P. J.; McLauchlan, K. A. *Chem. Phys. Lett.* **1997**, *272*, 376−382.
(19) Stass, D. V.; Woodward, J. R.; Timmel, C. R.; Hore, P. J.; McLauchlan, K. A. *Chem. Phys. Lett.* **2000**, *329*, 15−22.
(20) Timmel, C. R.; Woodward, J. R.; Hore, P. J.; McLauchlan, K. A.; Stass, D. V. *Meas. Sci. Technol.* **2001**, *12*, 635−643.
(21) Woodward, J. R.; Timmel, C. R.; McLauchlan, K. A.; Hore, P. J. *Phys. Rev. Lett.* **2001**, *87*, 077602/1−4.
(22) Woodward, J. R.; Timmel, C. R.; Hore, P. J.; McLauchlan, K. A. *Mol. Phys.* **2002**, *100*, 1181−1186.
(23) Bowman, M. K.; Budil, D. E.; Closs, G. L.; Kostka, A. G.; Wraight, C. A.; Norris, J. R. *Proc. Natl. Acad. Sci. U.S.A.* **1981**, *78*, 3305−3307.
(24) Frankevich, E. L.; Kubarev, S. I. In *Triplet state ODMR spectroscopy*; Clarke, R. H., Ed.; John Wiley: New York, 1982; pp 137−183.
(25) Lersch, W.; Michel-Beyerle, M. E. In *Advanced EPR. Applications in Biology and Biochemistry*; Hoff, A. J., Ed.; Elsevier, Amsterdam, 1989; pp 685−705.
(26) Levitt, M. H.; Eden, M. *Mol. Phys.* **1998**, *95*, 879−890.
(27) Hohwy, M.; Bildsoe, H.; Jakobsen, H. J.; Nielsen, N. C. *J. Magn. Reson.* **1999**, *136*, 6−14.
(28) Hodgkinson, P.; Emsley, L. *Prog. NMR Spectrosc.* **2000**, *36*, 201−239.
(29) Henbest, K. B.; Kukura, P.; Rodgers, C. T.; Hore, P. J.; Timmel, C. R. *J. Am. Chem. Soc.* **2004**, *126*, 8102−8103.
(30) Kaptein, R.; Oosterhoff, L. J. *Chem. Phys. Lett.* **1969**, *4*, 195−197.
(31) Bloch, F. *Phys. Rev.* **1956**, *102*, 104−135.
(32) Maricq, M. M.; Waugh, J. S. *J. Chem. Phys.* **1979**, *70*, 3300−3316.
(33) Eden, M.; Lee, Y. K.; Levitt, M. H. *J. Magn. Reson. A* **1996**, *120*, 56−71.
(34) Eden, M. *Concepts Magn. Reson. A* **2003**, *17*, 117−154.
(35) Eden, M. *Concepts Magn. Reson. A* **2003**, *18*, 1−23.
(36) Eden, M. *Concepts Magn. Reson. A* **2003**, *18*, 24−55.
(37) Levitt, M. H. *J. Magn. Reson.* **1989**, *82*, 427−433.
(38) Charpentier, T.; Fermon, C.; Virlet, J. *J. Magn. Reson.* **1998**, *132*, 181−190.
(39) Charpentier, T.; Fermon, C.; Virlet, J. *J. Chem. Phys.* **1998**, *109*, 3116−3130.
(40) There appears to be a slight error in eq 31 of ref 27, in which $\bar{a}_{rs}^{(k)}$ is given as $|q_{sr}^{(k)}|^2$. Equations 25−27 of ref 27, however, imply $\bar{a}_{rs}^{(k)} = |q_{rs}^{(k)}|^2$, which we believe to be correct.
(41) Lewis, I. C.; Singer, L. S. *J. Chem. Phys.* **1965**, *43*, 2712−27.
(42) Reiger, P. H.; Fraenkel, G. K. *J. Chem. Phys.* **1962**, *37*, 2795−2810.
(43) Schulten, K.; Wolynes, P. G. *J. Chem. Phys.* **1978**, *68*, 3292−3297.
(44) Morozov, V. A.; Doktorov, A. B. *Chem. Phys.* **1991**, *153*, 313−331.
(45) Morozov, V. A.; Doktorov, A. B. *Chem. Phys.* **1991**, *153*, 333−350.
(46) Bagryanskaya, E. G.; Yashiro, H.; Fedin, M.; Purtov, P.; Forbes, M. D. E. *J. Phys. Chem. A* **2002**, *106*, 2820−2828.
(47) Ponomarev, O. A.; Kubarev, S. I.; Kubareva, I. S.; Susak, I. P.; Shigaev, A. S. *Chem. Phys. Lett.* **2004**, *388*, 231−235.
(48) Ananchenko, G. S.; Potapenko, D. I.; Purtov, P. A.; Bagryanskaya, E. G.; Sagdeev, R. Z. *Appl. Magn. Reson.* **2004**, *26*, 65−82.
(49) Canfield, J. M.; Belford, R. L.; Debrunner, P. G.; Schulten, K. *Chem. Phys.* **1994**, *182*, 1−18.
(50) Canfield, J. M.; Belford, R. L.; Debrunner, P. G.; Schulten, K. *Chem. Phys.* **1995**, *195*, 59−69.
(51) Ivanov, K. L.; Vieth, H.-M.; Miesel, K.; Yurkovskaya, A. V.; Sagdeev, R. *Z. Phys. Chem. Chem. Phys.* **2003**, *5*, 3470−3480.
(52) Schulten, K.; Swenberg, C.; Weller, A. *Z. Phys. Chem. NF* **1978**, *111*, 1−5.
(53) Schulten, K. In *Festkörperprobleme*; Treusch, J., Ed.; Vieweg: Braunschweig, Germany, 1982; Vol. 22, pp 61−83.
(54) Schulten, K.; Windemuth, A. In *Biophysical Effects of Steady Magnetic Fields*; Maret, G., Kiepenheuer, J., Boccara, N., Eds.; Springer; Berlin, 1986; pp 99−106.
(55) Ritz, T.; Adem, S.; Schulten, K. *Biophys. J.* **2000**, *78*, 707−718.
(56) Ritz, T.; Thalau, P.; Phillips, J. B.; Wiltschko, R.; Wiltschko, W. *Nature (London)* **2003**, *429*, 177−180.